RSC Advances

This article can be cited before page numbers have been issued, to do this please use: B. Zou, H. Liu, J. Tian, J. Mack, Z. Li, H. Lu and Z. Shen, *RSC Adv.*, 2014, DOI: 10.1039/C4RA06416J.

ROYAL SOCIETY OF CHEMISTRY

www.rsc.org/advances

View Article Online
DOI: 10.1039/C4RA06416J

Journal Name

RSCPublishing

ARTICLE

A new aza-BODIPY based NIR region colorimetric and fluorescent chemodosimeter for fluoride

Cite this: DOI: 10.1039/xoxxooooox

Bin Zou,[a] Hui Liu,[a] John Mack,[c] Sisi Wang,[a] Jiangwei Tian,[b] Hua Lu,[a,]* Zhifang Li,[a] and Zhen Shen [b,]*

Received ooth January 2012,
Accepted ooth January 2012

DOI: 10.1039/xoxxooooox

www.rsc.org/

The synthesis and characterization of a novel NIR region fluoride sensor, that makes use of the aza-boron-dipyrromethene (aza-BODIPY) fluorophore, is described. An arylmagnesium bromide was formed by reacting 4-bromophenol with a *tert*-butyldimethylsilyl protecting group and magnesium, which was then used to prepare the aza-BODIPY through a reaction with phthalonitrile. The unusually strong affinity between the fluoride anion and silicon is used to create a sensor dye, which exhibits a highly specific, rapid colorimetric and 'turn-off' fluorescent response for F^- in solution and in living HeLa cells. Upon F^-, there is enhanced intramolecular charge transfer within the S_1 state and this results in efficient nonradiative decay and hence in a marked decrease in fluorescence emission intensity.

1. Introduction

In recent years, there has been considerable interest in developing efficient artificial receptors for molecular recognition and the sensing of biologically important anions that play indispensable roles in physiological processes.[1-4] The fluoride anion is one of the most significant in this regard due to its associated health and environmental issues. For example, fluoride deficiency causes poor dental health and osteoporosis, while overexposure may result in fluorosis and urolithiasis.[5-7] A number of fluorescent and/or chromogenic chemosensors have been designed for the fluoride anion.[8-13] Most have been based on hydrogen bonding or Lewis acid coordination and tend to be unsuitable for use in aqueous solution. In recent years that has been considerable interest in chemodosimeter approaches, which take advantage of the unusually strong affinity between fluoride and silicon.[14-17] These sensors have very high optical selectivity, fast response times and high sensitivity. Although various ratiometric, "turn-on" and "turn-off" fluorescent chemodosimeters have been investigated,[18-28] no example of emission in the near infrared (NIR) region has been reported to date, despite the fact that dyes that emit beyond 700 nm are more favorable for biological imaging applications, since environmentally induced light scattering is minimized, there is less photodamage and deeper tissue penetration during cell imaging is enabled.[29] The main goal of this study was to address this by making use of the aza-boron-dipyrromethene (aza-BODIPY) fluorophore. The potential utility of aza-boron-dipyrromethene (aza-BODIPY) fluorescent dyes, due to their favourable spectroscopic properties (such as high molar absorption coefficients, narrow and structured absorption and emission bands, small Stokes shifts, excellent photostability and their intense red/NIR region absorption and emission bands) has long been recognized.[29-31]

There have only been a few reports of aza-BODIPYs with sensor properties, since the absence of a *meso*-substituent limits the scope for ion binding and molecular recognition. Examples have included sensors for Hg^{2+},[32] NH_4^+,[33] *p*H,[34-38] cysteine, [39] and saxitoxin.[40]. Recently, the Shen and Kobayashi group reported a novel synthetic method for obtaining benzo-fused aza-BODIPYs through a two-step reaction of phthalonitrile and an arylmagnesium bromide.[38] Benzo-fused aza-BODIPYs have intense absorption and emission bands in the NIR region beyond 700 nm, with high molar absorption coefficients and moderately high fluorescence quantum yields. The spectroscopic properties make these compounds suitable for use as NIR sensors. With this in mind, a novel NIR region fluoride sensor, aza-BODIPY **1**, has been designed in a rational manner by taking advantage of the very strong affinity between fluoride and silicon, and its properties have been explored. Confocal fluorescence microscopy experiments demonstrate that **1** can successfully be used to monitor fluoride in living cells. Theoretical calculations have been used to investigate the reasons for the quenching of the fluorescence emission intensity upon F^-.

2. Experimental Section

2.1 Materials and Instrumentation.

All reagents were obtained from commercial suppliers and used without further purification unless otherwise indicated. All air and moisture-sensitive reactions were carried out under a nitrogen atmosphere. Benzene and THF were distilled over calcium hydride and sodium, respectively. Triethylamine was

View Article Online
DOI: 10.1039/C4RA06416D
Journal Name

obtained by simple distillation. Deionized distilled water was used throughout. NMR spectra were recorded on a Bruker DRX400 spectrometer and referenced to the residual proton signals of the solvent. Mass spectra were measured with a Bruker Daltonics AutoflexIITM MALDI–TOF spectrometer.

2.2. Synthesis

Synthesis of (4-bromophenoxy)(*tert*-butyl)dimethylsilane
4-Bromophenol (3 g, 17.3 mmol) and TBSCl (2.6 g, 17.3 mmol) in 30 mL of anhydrous THF was added to a Schlenk flask under argon. Et_3N (5 mL, 34.6 mmol) was then added dropwise into the mixture. The solvent was stirred overnight at room temperature. After completion of the reaction, the precipitate was removed by filtration and washed with dichloromethane. The organic fraction was collected, dried over sodium sulfate, concentrated under reduced pressure and purified through a silica-gel chromatography using petroleum ether as eluent to provide (4-bromophenoxy)(*tert*-butyl)dimethylsilane in 85% yield. ^{1}H NMR(400 MHz $CDCl_3$) δ = 0.23 (s, 6 H), 1.02 (s, 9 H), 6.75 (d, *J* = 8, 2 H), 7.36 (d, *J* = 12, 2 H).

Synthesis of aza-BODIPY **1**
A Grignard reagent was prepared from (4-bromophenoxy)(*tert*-butyl)dimethylsilane(4 g, 14 mmol) and magnesium turnings (400 mg, 16.7 mmol) in anhydrous THF. At room temperature, the Grignard reagent solution was then added to a vigorously stirring solution of phthalonitrile (5.6 mmol) in dry benzene (5 mL) and the resulting mixture was stirred for a further 1 h. The solvent was removed by using a rotary evaporator and the residue distilled with water steam, filtered, dried, and subsequently treated with $BF_3{\cdot}OEt_2$ in the presence of triethylamine in refluxing dry benzene. The crude product was purified through silica-gel chromatography (1:1 (v/v) CH_2Cl_2/petroleum ether as the eluent.) and recrystallized from CH_2Cl_2/hexane to provide aza-BODIPY **1** in 18% yield. ^{1}H NMR (400MHz,$CDCl_3$) δ = 0.28 (s, 12 H), 1.01 (s 18 H), 6.97 (d, *J* = 8, 4 H), 7.31 (d, *J* = 8, 2 H), 7.47−7.51 (t, 2 H), 7.66 (d, *J* = 8, 2 H), 7.83 (d, *J* = 8, 4 H), 8.10 (d, *J* = 8, 2 H); ^{13}C NMR (100 MHz, $CDCl_3$): δ 157.9, 133.5, 132.1, 131.1, 130.1, 126.8, 124.3, 123.4, 121.3, 120.0, 25.6, 18.2, -4.3; MALDI-TOF MS: m/z calcd for $[C_{40}H_{48}BF_2N_3O_2Si_2]^{+\bullet}$ m/z = 705.3, found m/z = 705.6 $[M]^+$, 686.8 $[M\text{-}F]^+$; HRMS-ESI: m/z: calcd $[C_{40}H_{47}BF_2N_3O_2Si_2+H]^+$ m/z = 706.3262, found m/z = 706.3266.

2.3 Spectroscopic Measurements

UV-visible absorption spectra were recorded on a Shimadzu 3000 spectrophotometer. Fluorescence spectra and lifetimes were measured on Horiba Jobin Yvon Fluorolog-3 spectrofluorimeter. Absorption and emission measurements were carried out in 1 × 1 cm quartz cuvettes. For all measurements, the temperature was kept constant at (298 ± 2) K. Dilute solutions with absorbance values of less than 0.05 at the excitation wavelength were used for the measurement of fluorescence quantum yields. Zinc phthalocyanine was used as the standard (Φ_F = 0.30 in benzene).[41] The quantum yield, Φ, was calculated using equation (1):

$$\Phi_{sample}=\Phi_{std}\left[\frac{I\,sample}{I\,std}\right]\left[\frac{A\,std}{A\,sample}\right]\left[\frac{nsample}{nstd}\right]^2 \quad (1)$$

where *sample* and *std* subscripts denote the sample and standard measurements, respectively, *I* is the integrated emission intensity, *A* stands for the absorbance, and *n* is the refractive index of the solvent.

2.4 Cell Culture and Confocal Imaging

The human cervical carcinoma HeLa cell line was obtained from the American Type Culture Collection (ATCC). HeLa cells were cultured in Dulbecco's modified Eagle's medium (DMEM) containing 10% fetal bovine serum (FBS), 100 μg mL^{-1} streptomycin and 100 U mL^{-1} penicillin at 37 °C in a humidified incubator containing 5% CO_2 and 95% air. The medium was replenished every second day and the cells were subcultured after reaching confluence. Confocal fluorescence imaging studies were performed on a confocal laser scanning microscope (CLSM; TCS SP5, Leica, Germany). Before imaging, the cells were rinsed three times with phosphate buffered saline. The cells were excited at 633 nm with a helium-neon laser and the emission was collected from 700□800 nm. All images were digitized and analyzed by Leica Application Suite Advanced Fluorescence (LAS-AF) software package.

2.5 Preparation of Solutions

Solutions of a series of ions (1 mM for Cl^-, Br^-, I^-, NO_2^-, NO_3^-, SCN^-, HSO_3^-, ClO_4^-, HSO_4^{2-}, HPO_4^{2-}, and $H_2PO_4^-$ and 10 mM, 1 mM for TBAF) were prepared in deionized water. In the titration experiments, a 2 mL solution of **1** was poured into a quartz optical cell with a 1 cm optical path length and the anion solution were then added using a micro-pipette. Spectral data were recorded immediately after each addition. For all measurements, the excitation and emission slit widths were set at 5 nm.

2.6 Theoretical Calculations

Geometry optimization and DFT calculations were carried out for a 3,5-diphenyl-aza-BODIPY (aza-BODIPY) model compound, **1** and its unprotected aza-BODIPY-O^{2-} dianion using the B3LYP functional of the Gaussian 09 software package [42] with 6-31G(d) basis sets. TD-DFT calculations were carried out in a similar by using the CAM-B3LYP functional, since TD-DFT calculations with the B3LYP functional are known to be problematic when significant charge transfer character is involved. [50,51]

3. Results and discussion

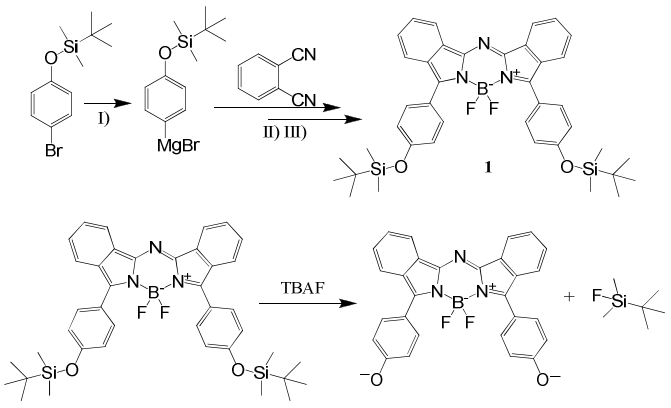

Scheme 1. Top: Synthesis and structure of aza-BODIPY **1**. I) Mg, THF, 2h; II) dry benzene, RT, 1h, water steam distillation; III) $BF_3{\cdot}Et_2O$, Et_3N, benzene, reflux. Bottom: F^- recognition mechanism.

View Article Online
DOI: 10.1039/C4RA06410B

Aza-BODIPY **1** was synthesized through the reaction of phthalonitrile with an arylmagnesium bromide (Scheme 1). The active hydroxyl group of the starting material was protected with a *tert*-butyldimethylsilyl group, and then reacted with magnesium to afford an arylmagnesium bromide, which was reacted with 1,2-dicyanobenzene to give product **1**. The new dye was characterized by high-resolution MALDI MS (HR-MS) and ^{1}H NMR spectroscopy. A molecular ion peak was observed at 706.3266 (calcd for $[M+H]^+$ = 706.3262) by HR-MS, and the isotopic pattern was in agreement with that calculated for the molecular structure. The absorption and fluorescence spectra of **1** (Fig. 1) are similar to those that have been reported previously for BODIPY sensors, [45-47] but there is a marked red-shift of the main spectral bands into the NIR region, due to the introduction of the aza-nitrogen atom. In CH_3CN, an intense S_0–S_1 band is observed at 718 nm and there is a pronounced shoulder of intensity at shorter wavelength at ca. 665 nm. The fluorescence spectrum exhibits mirror symmetry with the main absorption band with a maximum at 750 nm. The fluorescence quantum yield is 0.21 in CH_3CN. A fluorescence lifetime of 1.16 ns is obtained based on a single-exponential fit (Table 1).

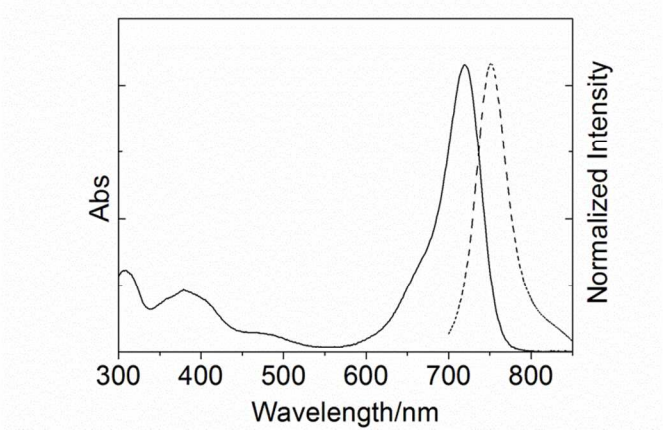

Fig. 1 Absorption and emission spectra of **1** in CH_3CN (λex = 680 nm).

Table 1 Spectroscopic properties of **1** and $[\mathbf{1\text{-}O_2}]^{2-}$ in CH_3CN at 298K

	λ_{abs} [nm]	λ_{em} [nm]	Φ_F	τ_F [ns]
1	718	750	0.21	1.16
$[\mathbf{1\text{-}O_2}]^{2-}$	780	ND	-	-

ND=Not Detected

The anion binding properties of **1** were investigated by monitoring changes in the fluorescence and UV-visible absorption spectra. Anion titration experiments were carried out in CH_3CN by adding 10 eq. of F^-, Cl^-, Br^-, I^-, NO_2^-, NO_3^-, HSO_3^-, SCN^-, ClO_4^-, HSO_4^-, HPO_4^{2-}, and $H_2PO_4^-$ into solutions of **1** (10 μM). When F^- was added, a significant decrease was observed in the intensity of the absorption band at 718 nm with a concomitant increase in the intensity of a new band at 780 nm. There is a sharp isosbestic point at 750 nm, and a visible color change from blue to indigo. The absorption band at 780 nm is the main absorption band of the unprotected dianion of **1** ($[\mathbf{1\text{-}O_2}]^{2-}$), which is red-shifted by 62 nm relative to that of aza-BODIPY **1**. Little or no change is observed in the absorption spectra of **1** in the presence of other anions (Fig. 2). The 780 nm band lies in the NIR region, and thus enables the colorimetric detection of F^- in the NIR region. The utility of aza-BODIPY **1** for fluorescence based detection of F^- has also been assessed. Pronounced quenching is immediately observed at 750 nm, due to a rapid reaction with F^-. Emission quenching is observed for **1** when F^- is added (Fig. 3). The emission peak at 750 nm gradually decreases in intensity as the amount of F^- is increased, the fluorescence intensity decreased linearly with added fluoride concentration (Fig. 3 inset). The detection limit towards F^- is evaluated to be 40 ppb, which was well below 4 ppm, the allowed concentration level of F^- in drinking water specified by USEPA.[52] There is no obvious change in the fluorescence intensity upon addition of 10 eq. of Cl^-, Br^-, I^-, NO_2^-, NO_3^-, SCN^-, HSO_3^-, ClO_4^-, HSO_4^-, HPO_4^{2-}, and $H_2PO_4^-$ (Fig. 3). These results demonstrate that **1** can act with high selectivity as a dual-signal chemosensor for F^-. Howover, emission and absorption spectra almost unchanged by addition of 10 eqiv. F^- to the solution of compound **1** in the presence of the other anions such as Br^-, I^-, NO_2^-, NO_3^-, HSO_3^-, SCN^-, ClO_4^-, HSO_4^-, HPO_4^{2-}, and $H_2PO_4^-$, this meaning most of anion interfere in the F^- response.

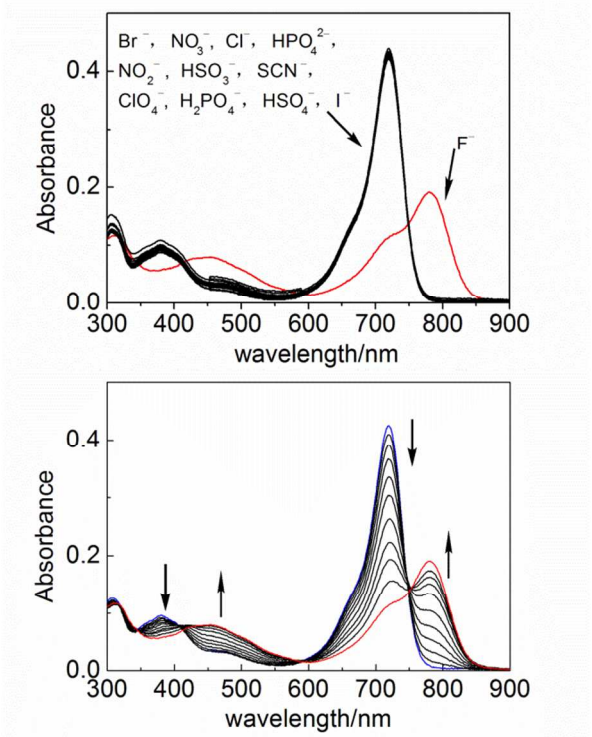

Fig. 2 Top: Absorption spectra of **1** (10 μM) in CH_3CN after the addition of 10 equiv. of various anions. Bottom: Absorption spectra of **1** (10 μM) in CH_3CN after the addition of TBAF.

View Article Online
DOI: 10.1039/C4RA06410D
Journal Name

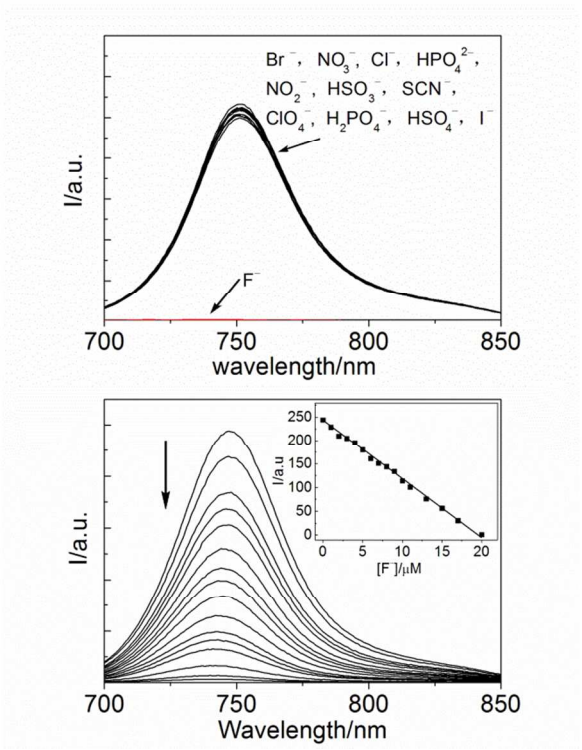

Fig. 3 Top: Fluorescence response of **1** (10 μM) in CH3CN after the addition of 10 equiv. of various anions. Bottom: Fluorescence spectra of **1** (10 μM) in CH_3CN after the addition of TBAF (λex = 680 nm). Inset: Plot of emission intensity versus TBAF concentration. Fluorescence measurements were performed immediately after adding TBAF to 1.

Upon reaction with F^- anions, the *tert*-butyldimethylsilyl group of **1** are removed to form the unprotected $\mathbf{[1\text{-}O_2]^{2-}}$ dianion. This can be expected to result in significant differences in the electronic structure and hence also in the photophysical properties. DFT and TD-DFT calculations were carried out for 1 and $\mathbf{[1\text{-}O_2]^{2-}}$ at the B3LYP/6-31G(d) level of theory to obtain an in-depth insight into the spectroscopic properties (Figs. 4–6).

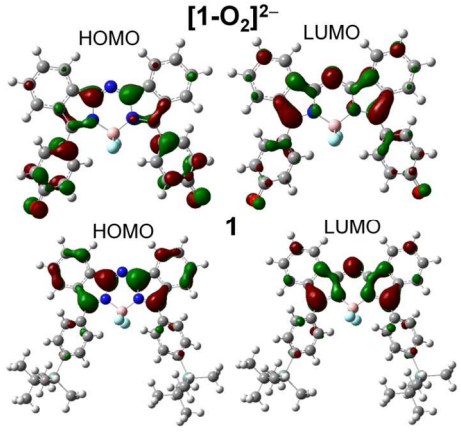

Fig. 4 The frontier π-MOs of aza-BODIPY **1** and $\mathbf{[1\text{-}O_2]^{2-}}$ at an isosurface value of 0.04 a.u., calculated during TD-DFT calculations using the CAM-B3LYP functional with 6-31G(d) basis sets.

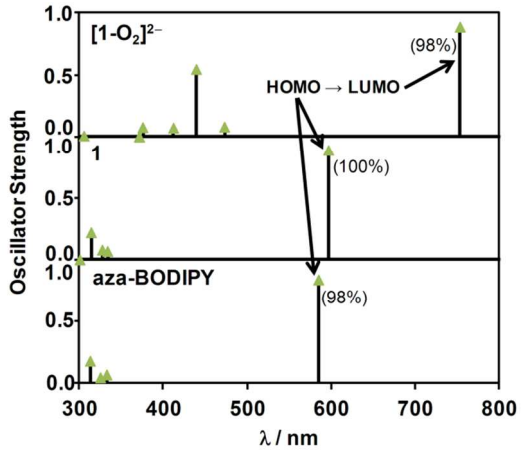

Fig. 5 TD-DFT spectra calculated for a 3,5-diphenyl-aza-BODIPY (aza-BODIPY) model compound, **1** and $\mathbf{[1\text{-}O_2]^{2-}}$. The main absorption band in each case is almost entirely associated with the HOMO → LUMO one-electron transition.

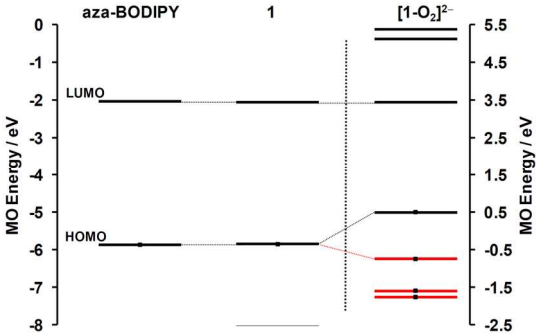

Fig. 6 The energies of the frontier π-MOs calculated for a 3,5-diphenyl-aza-BODIPY (aza-BODIPY) model compound, **1** and $\mathbf{[1\text{-}O_2]^{2-}}$ during TD-DFT calculations using the CAM-B3LYP functional with 6-31G(d) basis sets. Black squares are used to highlight occupied MOs, and red lines are used to highlight MOs primarily associated with the peripheral oxygen atoms. The MO energies for $\mathbf{[1\text{-}O_2]^{2-}}$ are plotted against a secondary axis.

The HOMO and LUMO of **1** are mainly delocalized on the aza-BODIPY core (Fig. 4). In contrast, the HOMO of $\mathbf{[1\text{-}O_2]^{2-}}$ has significant MO coefficients on the 3,5-substituted phenoxy group and the pyrrole moieties, with smaller coefficients on the benzo rings, while the largest MO coefficients of the LUMO are confined to the core aza-BODIPY fluorophore. The S_1 excited state for $\mathbf{[1\text{-}O_2]^{2-}}$, therefore, has significant intramolecular charge transfer from the electron donating phenoxy moiety to the BODIPY core (Fig. 4). An intramolecular charge transfer mechanism is, therefore, the most probable explanation for the colorimetric response and fluorescent quenching of **1**. The presence of electron donating phenoxide ions, destabilizes the HOMO, and narrows the HOMO–LUMO gap (Fig. 6), and thus results in a large red shift of the main absorption band in both the calculated and observed spectra (Figs. 2 and 5). There is still significant

View Article Online
DOI: 10.1039/C4RA06410B ARTICLE

overlap between the HOMO and LUMO, however, so the main S_0–S_1 absorption band of $[\mathbf{1}\text{-}\mathbf{O_2}]^{2-}$ is predicted to retain significant intensity (Figs. 4 and 5). The efficient nonradiative relaxation is probably caused by conical intersections formed between the potential-energy surfaces of the S_1 excited state and the ground state.[48,49] The spectroscopic behavior of $[\mathbf{1}\text{-}\mathbf{O_2}]^{2-}$ is similar to that of aza-BODIPYs with $-N(CH_3)_2$ substituents, which are believed to result in an intense intramolecular charge transfer process from the electron donating dimethylamino group to the electron-deficient aza-BODIPY core.[38]

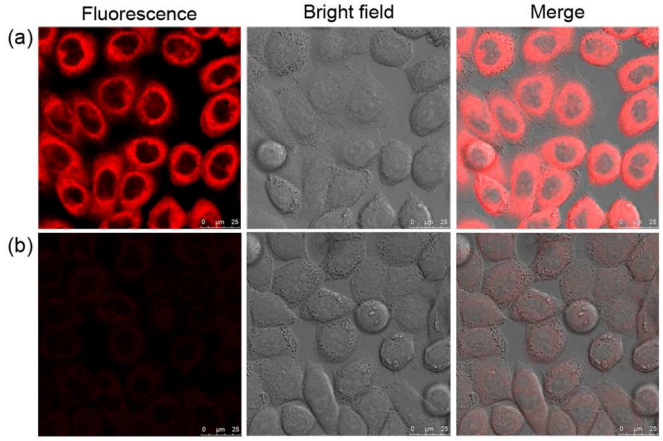

Fig. 7 Confocal fluorescence images of aza-BODIPY **1**-incubated HeLa cells in the absence (a) and presence (b) of TBAF (λ_{ex} = 633 nm). Hela cells were incubated with 10 μM aza-BODIPY **1** for 1 h at 37 °C. For F^- imaging, the aza-BODIPY **1**-incubated Hela cells were subsequently incubated with 100 μM TBAF for 1 h at 37 °C.

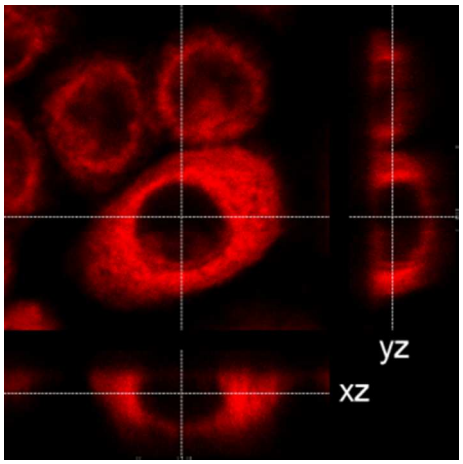

Fig. 8 Three-dimensional fluorescence image of living Hela cells incubated with 10 μM aza-BODIPY **1** for 1 h at 37 °C (λ_{ex} = 633 nm).

The practical utility of **1** as a fluoride probe in living cells has also been evaluated by carrying out experiments with living HeLa cells. Upon incubation with 10 μM of **1** for 30 min at 37 °C, the cells display strong intracellular fluorescence in the NIR region. Further treatment with F^- for 1 h in the culture medium, followed by washing with phosphate buffered saline to remove extracellular F^-, resulted in the disappearance of the bright red fluorescence image in these cells. Brightfield measurements after treatment with both F^- and **1** confirm that the cells were viable throughout the imaging experiments. The overlay of fluorescence and brightfield images reveals that the fluorescence signals are localized in the perinuclear region of the cytosol, indicating weak nuclear uptake and exclusive staining in the cytoplasm (Fig. 7). This was also confirmed by Z-scan luminescence imaging of HeLa cells stained with **1** (Fig. 8). The results demonstrate that **1** is cell-permeable and can respond effectively to variations in the concentration of intracellular F^-.

4. Conclusion

In summary, an NIR region aza-BODIPY derivative, **1**, has been synthesized and characterized, which exhibits high selectivity toward F^- relative to various other inorganic anions and bio-relevant analytes, due to the strong affinity of F^- toward silicon. The quenching of the fluorescence intensity upon addition of F^- can be attributed to the intramolecular charge transfer character of the S_1 state, since this can greatly enhance the rate of nonradiative decay. Confocal fluorescence microscopy experiments have established the utility of **1** for monitoring the presence of F^- in living cells.

Acknowledgments

This research was financially supported by NSFC (no. 21471042). Zhejiang Provincial Natural Science Foundation of China (No. LY14B010003). Theoretical calculations were carried out at the Computational Center for Molecular Design of Organosilicon Compounds, Hangzhou Normal University and at the Centre for High Performance Computing in Cape Town

Notes

[a] *Key Laboratory of Organosilicon Chemistry and Material Technology, Ministry of Education, Hangzhou Normal University, Hangzhou, 310012, P. R. China. Email:hualu@hznu.edu.cn*

[b] *State Key Laboratory of Coordination Chemistry, School of Chemistry and Chemical Engineering, Nanjing University, Nanjing, 210093, P. R. China.*

[c] *Department of Chemistry, Rhodes University, Grahamstown 6140, South Africa.*

references

1 Z. Liu, W. He and Z. Guo, *Chem. Soc. Rev.*, 2013, **42**, 1568–1600.
2 P. A. Gale, *Chem. Soc. Rev.*, 2010, **39**, 3746–3771.
3 J. L. Sessler, P. A. Gale and W. S. Cho, Anion Receptor Chemistry, Cambridge: RSC Publishing Company, 2006.
4 P. A. Gale, *Chem. Commun.*, 2011, **47**, 82–86.
5 J. Fawell, K. Bailey, J. Chilton, E. Dahi, L. Fewtrell and Y. Magara, Fluoride in Drinking Water, WHO Drinking-Water Quality Series, IWA Publishing, London, UK and Seattle, USA, 2006.

View Article Online
DOI: 10.1039/C4RA06416D
Journal Name

6 E. B. Bassin, D. Wypij and R. B. Davis, *Cancer Causes. Control.*, 2006, **17**, 421–428.
7 H. S. Horowitz, *J. Publ. Health. Dent.*, 2003, **63**, 183–188.
8 M. R. Martínez and F. Sancenón, *Coord. Chem. Rev.*, 2006, **250**, 3081–3093.
9 T. Mizuno, W. H. Wei, L. R. Eller and J. L. Sessler, *J. Am. Chem. Soc.*, 2002, **124**, 1134–1135.
10 Q. Wang, Y. Xie, Y. Ding, X. Li and W. Zhu, *Chem. Commun.*, 2010, **46**, 3669–3671.
11 C. R. Wade, A .E. J. Broomsgrove, S. Aldridge and F. P. Gabbai, *Chem. Rev.*, 2010, 110, 3958–3984.
12 H. Li, R .A. Lalancette and F. Jäkle, *Chem. Commun.*, 2011, **47**, 9378–9380.
13 R. M. Duke, E. B. Veale, F. M. Pfeffer, P. E. Kruger and T. Gunnlaugsson, *Chem. Soc. Rev.*, 2010, **39**, 3936–3953.
14 J. Du, M. Hu, J. Fan and X. Peng, *Chem. Soc. Rev.*, 2012, **41**, 4511–4535.
15 K. Kaur, R. Saini, A. Kumar, V. Luxami, N. Kaur, P. Singh and S. *Coord. Chem. Rev.*, 2012, **256**, 1992–2028.
16 D. G. Cho and J. L. Sessler, *Chem. Soc. Rev.*, 2009, **38**, 1647–1662.
17 Y. Bao and R. Bai, *Progress in Chem.*, 2013, **25**, 288–295.
18 L. Gai, H. Chen, B. Zou, H. Lu, G. Lai, Z. Li and Z. Shen, *Chem. Commun.*, 2012, **48**, 10721–10723.
19 H. Lu, Q. Wang, Z. Li, G. Lai, J. Jiang and Z. Shen, *Org. Biommol. Chem.*, 2011, **9**, 4558–4562.
20 X. Cao, W. Lin, Q. Yu and J. Wang, *Org. Lett.*, 2011, **13**, 6098–6101.
21 Y. Bao, B. Liu, H. Wang, J. Tian and R. Bai, *Chem. Commun.*, 2011, **47**, 3957–3959.
22 B. Zhu, F. Yuan, R. Li, Y. Li, Q. Wei, Z. Ma, B. Du and X. Zhang, *Chem. Commun.*, 2011, **47**, 7098–7100.
23 O.A. Bozdemir, F. Sozmen, O. Buyukcakir, R. Guliyev, Y. Cakmak and E. U. Akkaya, *Org. Lett.*, 2010, **12**, 1400–1403.
24 F. Zheng, F. Zeng, C. Yu, X. Hou and S. Wu, *Chem. Eur. J.*, 2013, **19**, 936–942.
J. F. Zhang, C. S. Lim, S. Bhuniya, B. R. Cho and J. S. Kim, *Org. Lett.*, 2011, **13**, 1190–1193.
25 X. Song, P. Hou, S. Chen, H. Wang, K. Voitchovsky and J. Wang, *Chem. Commun.*, 2014, **50**, 320–322.
26 D. Kim, S. Singh, T. Wang, E. Seo, J. H. Lee, S .J. Lee, K. H. Kim and K. H. Ahn, *Chem. Commun.*, 2012, **48**, 10243–10245.
27 S. Yang, Y. Liu and G. Feng, *RSC Adv.*, 2013, **3**, 20171–20178.
28 J. Cao, C. Zhao, P. Feng, Y. Zhang and W. Zhu, *RSC Adv.*, 2012, **2**, 418–420.
29 H. Liu, H. Lu, J. Xu, Z. Liu, Z. Li, J. Mack and Z. Shen, *Chem. Commun.,* 2014, **50**, 1074–1076.
30 H. Lu, J. Mack, Y.o Yang, and Z. Shen, *Chem. Soc. Rev.,* 2014, **43**, 4778–823.
31 W. Zhao and E. M. Carreira, *Angew. Chem. Inter. Ed.*, 2005, **44**, 1677–1679.
32 A. Coskun, M. D. Yilmaz and E. U. Akkaya, *Org. Lett.*, 2007, **9**, 607–609.
33 H. Liu, J. Mack, Q. Guo, H. Lu, N. Kobayashi and Z. Shen, *Chem. Commun.*, 2011, **47**, 12092–12094.
34 J. Murtagh, D. O. Frimannsson and D. F. O'Shea, *Org. Lett.*, 2009, **11**, 5386–5389.
35 A. Palma, M. Tasior, D. O. Frimannsson, T. T. Vu, R. M. Renault and D. F. O'Shea, *Org. Lett.*, 2007, **9**, 3638–3641.
36 J. Killoran, S. O. McDonnell, J. F. Gallagher, D. F. O'Shea, *New J. Chem.*, 2008, **32**, 483–489.
37 J. Killoran and D. F. O'Shea, *Chem. Commun.*, 2006, **42**, 1503–1505.
38 H. Lu, S. Shimizu, J. Mack, Z. Shen and N. Kobayashi, *Chem. Asian J.*, 2011, **6**, 1026–1037.
39 X. D. Jiang, J. Zhang, X. Shao and W. Zhao, *Org. Biommol. Chem.*, 2012, **10**, 1966–1968.
40 R. E. Gawley, H. Mao, M. M. Haque, J. B. Thorne and J. S. Pharr, *J. Org. Chem.*, 2007, **72**, 2187–2191.
41 A. M. Brouwer, *Pure Appl. Chem.*, 2011, **83**, 2213–2228.
42 Gaussian 09, Revision D.01, M. J. Frisch, G. W. Trucks, H. B. Schlegel, G. E. Scuseria, M. A. Robb, J. R. Cheeseman, G. Scalmani, V. Barone, B. Mennucci, G. A. Petersson, H. Nakatsuji, M. Caricato, X. Li, H. P. Hratchian, A. F. Izmaylov, J. Bloino, G. Zheng, J. L. Sonnenberg, M. Hada, M. Ehara, K. Toyota, R. Fukuda, J. Hasegawa, M. Ishida, T. Nakajima, Y. Honda, O. Kitao, H. Nakai, T. Vreven, J. A. Montgomery, Jr., J. E. Peralta, F. Ogliaro, M. Bearpark, J. J. Heyd, E. Brothers, K. N. Kudin, V. N. Staroverov, R. Kobayashi, J. Normand, K. Raghavachari, A. Rendell, J. C. Burant, S S. Iyengar, J. Tomasi, M. Cossi, N. Rega, J. M. Millam, M. Klene, J. E. Knox, J. B. Cross, V. Bakken, C. Adamo, J. Jaramillo, R. Gomperts, R. E. Stratmann, O. Yazyev, A. J. Austin, R. Cammi, C. Pomelli, J. W. Ochterski, R. L. Martin, K. Morokuma, V. G. Zakrzewski, G. A. Voth, P. Salvador, J. J. Dannenberg, S. Dapprich, A. D. Daniels, Ö. Farkas, J. B. Foresman, J. V. Ortiz, J. Cioslowski, D. J. Fox, Gaussian, Inc., Wallingford CT, 2009.
43 R. J. Magyar and S. J. Tretiak, *J. Chem. Theo. Comp.*, 2007, **3**, 976–987.
44 Z. L. Cai, M. J. Crossley, J. R. Reimers and R. Kobayashi, *J. Phys. Chem. B* 2006, **110**, 15624–15632.
45 L. Gai, J. Mack, H. Liu, Z. Xu, H. Lu and Z. Li, *Sensors Actuators B-Chem.,* 2013, **182**, 1–6.
46 H. Lu, L. Xiong, H. Liu, M. Yu, Z. Shen, F. Li and X. You, *Org. Biommol. Chem.*, 2009, **7**, 2554–2558.
47 H. Lu, Q. Wang, L. Gai, Z. Li, Y. Deng, X. Xiao, G. Lai and Z. Shen, *Chem. Eur. J.*, 2012, **18**, 7852–7861.
48 H. Lu, Z. L. Xue, J. Mack, Z. Shen, X. Z. You and N. Kobayashi, *Chem. Commun.*, 2010,**46**, 3565–3567.
49 L. Gai, J. Mack, H. Lu, H. Yamada, D. Kuzuhara, G. Lai,Z. Li, Z. Shen, *Chem. Eur. J.*, 2014, **21**, 1091–1102.
50 G. I. Jones, S. Kumar, O. Klueva and D. Pacheco, *J. Phys. Chem. A*, 2003, **107**, 8429–8434.
51 Z. R. Grabowski, K. Rotkiewicz and W. Rettig, *Chem. Rev.*, 2003, **103**, 3899–4031.
52 J. Fawell, K. Bailey, J. Chilton, E. Dahi, L. Fewtrell and Y. Magara, Fluoride in Drinking Water, WHO Drinking-Water Quality Series, IWA Publishing, London, UK, Seattle, USA, 2006.

View Article Online
DOI: 10.1039/C4RA06416J

GRAPHIC ABSTRACT

The synthesis and characterization of a NIR region fluoride anion sensor based on aza-BODIPY fluorophore, is described.